

Chapter 5



Journal of The Electrochemical Society



ACCEPTED MANUSCRIPT

Sensitive Electrochemical Determination of Creatinine in Human Serum Based on its Complexation with Cobalt Ion

Nayab Hussain, Uddipana Saikia, Pradyut Acharjee and Panchanan Puzari

Accepted Manuscript online 18 March 2025 • © 2025 The Electrochemical Society ("ECS"). Published on behalf of ECS by IOP Publishing Limited. All rights, including for text and data mining, AI training, and similar technologies, are reserved.

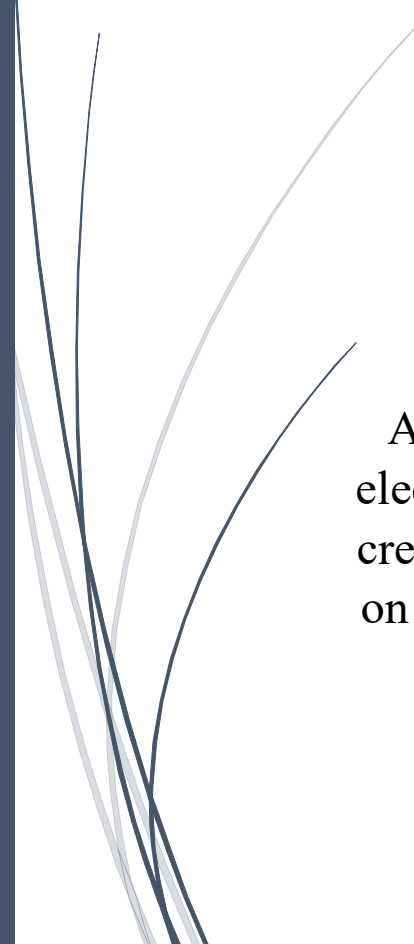
[What is an Accepted Manuscript?](#)

DOI 10.1149/1945-7111/adc208

Permissions

[Get permission to re-use this article](#)

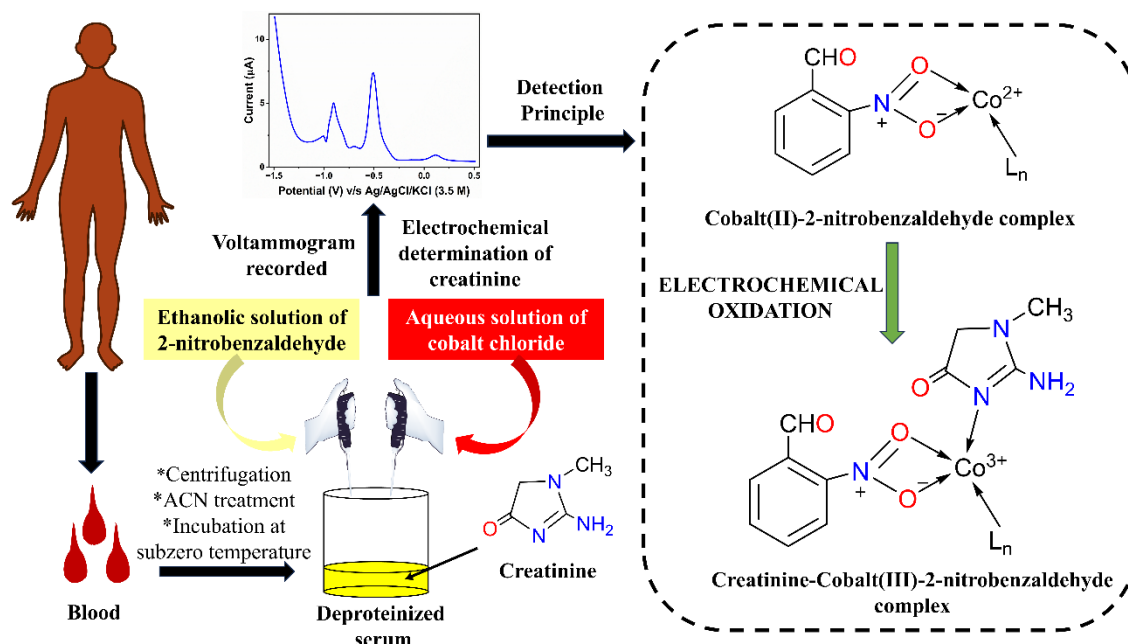
Share this article



A highly selective method for electrochemical determination of creatinine in human serum based on its coordination reaction with Co^{3+} in the presence of 2-nitrobenzaldehyde

Highlights

This chapter focuses on developing a new method for creatinine determination, based on its direct coordinating property with cobalt ions, which is an underexplored avenue in the development of electrochemical creatinine-sensing approaches. The addition of creatinine to the Co^{2+} -2-nitrobenzaldehyde complex converts the latter to a Co^{3+} complex, triggering a voltammetric response. This response has been utilized to develop a non-enzymatic creatinine determination method, using the Differential Pulse Voltammetry technique. A reaction time of 5 minutes, a 2-nitrobenzaldehyde concentration of 7 % (weight/volume in ethanol), and a cobalt chloride concentration of 0.5 M were determined to be the optimum parameters. The system exhibited excellent linearity in the concentration range of 50 μM to 600 μM , with an R^2 value of 0.99 and an LOD of 9.5 μM . Interference study was carried out with different serum components and the applicability of this method was demonstrated successfully in deproteinized human serum. From electrochemical analysis, supported by spectroscopic findings, a plausible reaction mechanism has also been proposed and all the redox peaks were designated.



This part of the thesis is published as:

Hussain, N., Saikia, U., Acharjee, P. and Puzari, P. Sensitive electrochemical determination of creatinine in human serum based on its complexation with cobalt ion. *Journal of The Electrochemical Society*, 2025. DOI: <https://doi.org/10.1149/1945-7111/adc208>

5.1 Introduction

Although creatinine's coordination with copper, silver, and iron ions has been extensively explored for electrochemical sensing of creatinine, the well-documented interaction between creatinine and cobalt ions [1, 2] remains largely untapped in this context. In 2020, *Dasgupta et al.* [3] reported the usage of cobalt ions for developing an electrochemical serum creatinine determination method. However, the method proposed by *Dasgupta et al.* [3] was not based on the direct coordination of cobalt ions with creatinine, but rather on an interesting enzymatic transformation of creatinine to 1-methylhydantoin, followed by its complexation with cobalt ions.

In Chapter 3, we proposed the formation of oxalylmethylguanidine, as an electrochemical oxidation product in the reaction between creatinine, 2-nitrobenzaldehyde (2-NBA) and NaOH. Due to the similarity in the chemical structures and coordinating sites in 1-methylhydantoin and oxalylmethylguanidine, it occurred to us that complexation of cobalt ions with oxalylmethylguanidine was possible, which could enable us to develop a more sensitive creatinine determination method. However, in Chapter 4, we discovered that the combination of creatinine, cobalt ions and 2-NBA yields a creatinine- Co^{3+} -2-NBA complex. This complexation process also opened up a new route for creatinine determination, as we observed that the interaction of creatinine with a Co^{2+} -2-NBA mixture triggers the conversion of Co^{2+} to Co^{3+} .

Hence, in this work, we have studied the reaction between creatinine, 2-NBA, and the cobalt ion in the buffer medium from an electrochemical perspective to develop a serum creatinine detection method. The reaction conditions were optimized for efficiency, interference studies were carried out and a real sample (serum) analysis was accomplished. Furthermore, a plausible mechanistic route and designation of all the redox processes have also been presented in this work.

5.2 Experimental

5.2.1 Chemicals, reagents and instruments

Creatinine (98%) was procured from Alfa Aesar; cobalt chloride hexahydrate from Sigma Aldrich; ethanol, potassium chloride, uric acid (99%, crystalline), ascorbic acid, glucose (anhydrous) and acetonitrile from Merck; dipotassium hydrogen phosphate, 2-

nitrobenzaldehyde (extra pure analytical reagent) and urea (extra pure) from SRL; and potassium dihydrogen phosphate from Rankem. All these chemicals were of analytical grade and were used without further purification.

Phosphate buffer saline (PBS) of 0.1 M strength was used.

For electrochemical analyses, Biologic SP-300 with EC-lab software setup was used. UV-visible spectroscopy was carried out using UV-2600I (Shimadzu). REMI R-8C model was used for centrifugation.

5.2.2 Solution preparation

Creatinine solutions (abbreviated as CRS) were prepared in PBS (phosphate buffer saline) of pH 7.4 (physiological pH). 2-NBA solutions having different weight/volume percentages (%) were prepared in ethanol and cobalt chloride solutions (abbreviated as 'CCS') having different molar (M) concentrations were prepared in Milli-Q water. The mixture of PBS, 2-NBA solution and CCS in a 100:1:1 volume ratio will be referred to as the 'blank solution' or abbreviated as PBS/2-NBA/CCS. The mixture of CRS, 2-NBA solution and CCS in a 100:1:1 volume will be referred to as the 'test solution' or abbreviated as CRS/2-NBA/CCS. Unless stated otherwise, the volume ratios mentioned above have been maintained throughout the work.

5.2.3 Electrochemical and spectroscopic procedures

For electrochemical analyses, 10 μl of 2-NBA solution and 10 μl of CCS were added to 1000 μl of PBS (in case of blank solution analysis), CRS or human blood serum (HBS), and transferred to the electrochemical cell for the analyses.

The differential pulse voltammetry (DPV) technique was employed to electrochemically investigate the reaction between creatinine, 2-NBA and cobalt ions. Reaction optimization, limit of detection (LOD) determination, interference study, real sample analysis, and deduction of a plausible mechanism were carried out using the DPV technique. For all the electrochemical analyses, a well-polished bare glassy carbon electrode was used as the working electrode, Ag/AgCl/KCl (3.5 M) as the reference electrode and Pt wire as the counter electrode. DPVs were recorded in the potential window of -1.35 V to 0.5 V with a pulse height of 2.5 mV , pulse width of 100 ms , step height of 5.0 mV , and step time of 500 ms .

Further evidence to support the proposed mechanistic pathway was sought through UV-visible spectroscopic analysis, which was performed across a wavelength range of 200–800 nm.

5.2.4 Optimization of reaction parameters

For reaction time optimization, triplicate DPVs were recorded for test solutions after different reaction times, keeping the concentration of 2-NBA, CRS (0.5 mM) and CCS fixed. Similarly, for optimizing the concentrations of 2-NBA and CCS, triplicate DPV measurements were recorded for test solutions with varying the concentration of the solution (CCS or 2-NBA solution) that needed to be optimized, while keeping the concentration of the other parameters constant. The optimum parameters (reaction time and concentrations) were then determined from the respective graphs of the average oxidative peak currents plotted against different reaction times and concentrations.

5.2.5 Electrochemical determination of creatinine and LOD calculation

Triplicate DPVs were recorded for each test solution while maintaining optimum reaction conditions and varying the creatinine concentration. The concentration of CRS added to prepare the test solution was varied from 0.05 mM to 1 mM. From the graph of average oxidative peak currents plotted against the different concentrations of creatinine, a calibration curve was obtained with a slope of 'm' for its linear range. Triplicate DPVs were also recorded for the blank solution and the standard deviation of the blank (S_b) was calculated from the oxidative peak currents measured in the absence of the analyte. The LOD of the system was then calculated with the formula:

$$\text{LOD} = 3(S_b/m)$$

5.2.6 Interference

Average oxidative peak current (C_1) was determined for interferent-free test solution having 0.1 mM creatinine in the added CRS, after recording triplicate DPVs at optimum conditions. Triplicate DPVs were also recorded at optimum conditions for test solutions having the same creatinine concentration, spiked with different concentrations of probable interferents (uric acid, ascorbic acid, glucose, urea, and albumin), and the average oxidative peak current (C_2) in each case was determined. The percentage of interference (I) for each spiked component was calculated by using the formula:

$$I = [(C1-C2)/C1] * 100 \%$$

5.2.7 Serum sample collection and deproteinization

Waste HBS was collected from *Health Centre, Tezpur University*. The HBS sample was treated with acetonitrile (ACN) to precipitate out the high molecular weight proteins [50, 51] and an HBS-ACN ratio of 1:2 was maintained which is efficient for protein precipitation [51]. The mixture was then vortexed for 30 seconds and centrifuged for 10 minutes at 5200 rpm to obtain the protein precipitate. The mixture was subsequently incubated at $-20\text{ }^{\circ}\text{C}$ for 1 hour to separate ACN and the deproteinized HBS [4]. ACN accumulated at the top layer, which was separated out and the deproteinized serum was carefully collected for analysis. The process to obtain the deproteinized HBS is illustrated in Figure 5.1.

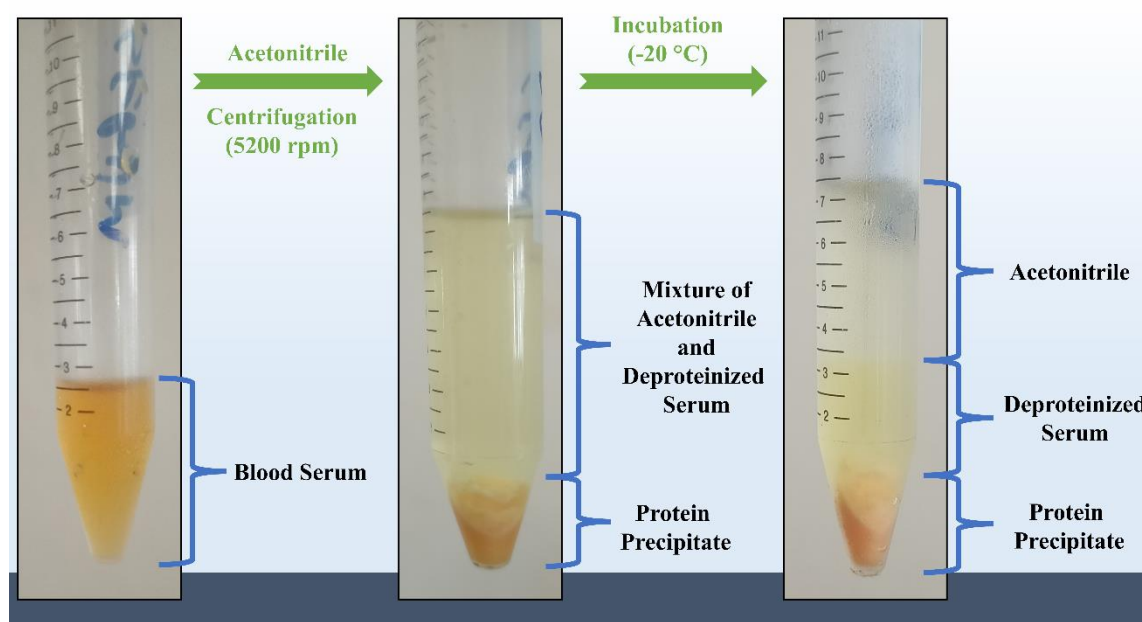


Figure 5.1: Illustration of the process to obtain deproteinized serum.

Triplicate DPVs were recorded at optimum conditions for 6-fold diluted (with PBS of pH 7.4) deproteinized HBS mixed with CCS and 2-NBA solution. Triplicate DPVs were also recorded for the deproteinized HBS sample spiked with different concentrations of creatinine after the addition of CCS and 2-NBA solution, and the creatinine recovery percentage in each case was calculated.

5.3 Results and Discussion

5.3.1 Electrochemical behaviour

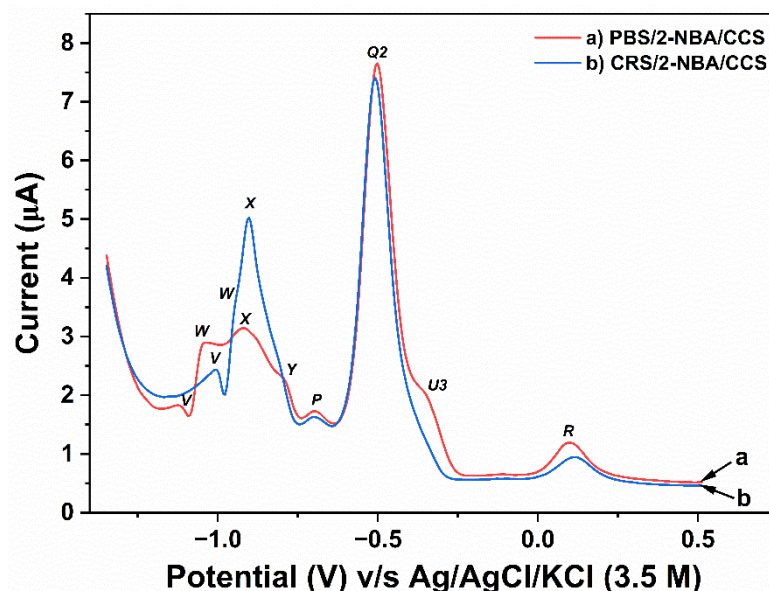


Figure 5.2: DPVs obtained for a) blank solution (PBS/2-NBA/CCS) and b) test solution (CRS/2-NBA/CCS).

Figure 5.2 represents the DPVs obtained for the blank and the test solution. The concentration of CRS added to prepare the test solution was 0.5 mM. As can be seen in Figure 2, multiple oxidation peaks, assigned as *V*, *W*, *X*, *Y*, *P*, *Q2*, *U3* and *R*, were obtained for the blank solution (curve a). However, several changes in the voltammogram were observed for the test solution (curve b). On comparing the peak positions, while a slight shift towards the positive potentials was observed for peaks *V* and *W* in the presence of creatinine, no such peak shift was marked for *X*, *Y*, *P*, *Q2* and *R*. Furthermore, the peaks *W* and *Y* appeared feebly to be distinguished properly. On comparing the peak intensities, it was seen that while the peaks *V*, *W* and *X* intensified to different extents in the presence of creatinine, the intensity of peak *U3* was found to be inhibited and the other peaks (*Y*, *P*, *Q2* and *R*) showed no considerable changes. The shifting and masking of these oxidation peaks are explained in Section 5.3.3 and all the involved oxidation processes are explained in detail in Section 5.3.6.

The intensification and inhibition of some peaks in the test solution as compared to the corresponding peaks in the blank solution, are a strong indication of certain reactions

driven by the presence of creatinine. Amongst the peaks which got intensified in the presence of creatinine, peak X was found to vary quantitatively with creatinine concentration. Hence, the intensity variation of X was considered for all the proceeding optimization steps and electrochemical analyses.

5.3.2 Optimization of the reaction time and concentration of the reagents

The optimization of the reaction time and the concentrations of the reagents present in the solution mixture are required for the efficient determination of the analyte (creatinine). The results of the optimization of the reaction time, concentration of CCS, and concentration of 2-NBA solution are shown in Figures 5.3 through 5.5.

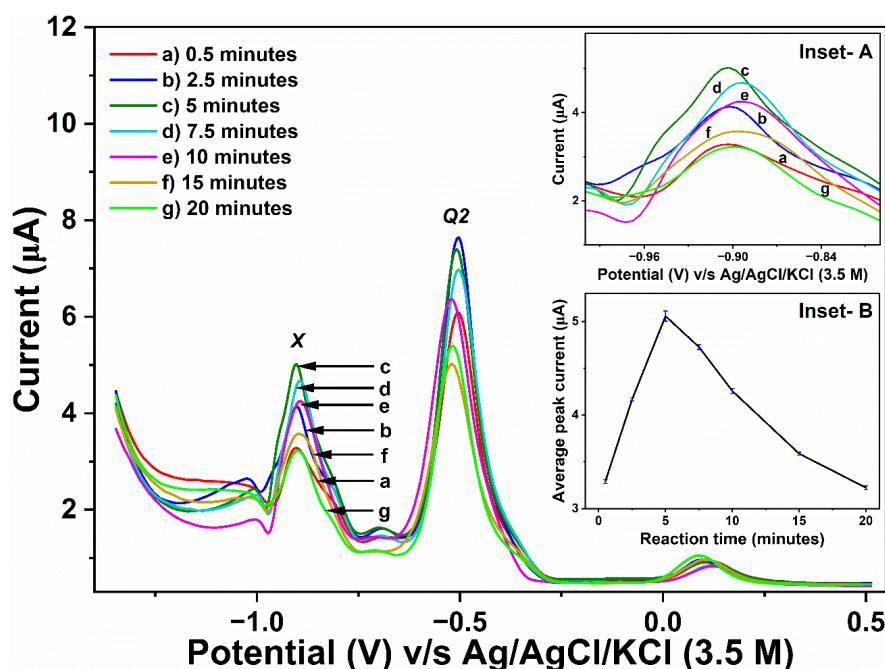


Figure 5.3: DPVs obtained for test solutions after different reaction times ('Inset- A' shows the enlarged view of peak X . 'Inset- B' represents the plot of peak X intensity v/s reaction time).

Figure 5.3 represents the DPVs obtained for test solutions after different reaction times while keeping the concentrations of 2-NBA, CRS and CCS fixed. From the calibration curve of the average oxidative peak current of X plotted against different reaction times, shown in Figure 5.3 (Inset- B), it was observed that the intensity of X initially increased as we increased the reaction time from 0.5 minutes to 5 minutes and thereafter, it showed a sharp decreasing trend. It is presumed that the electrochemical

oxidation and the creatinine-cobalt coordination are simultaneous processes, during which a spatial rearrangement of the ligands around the Co^{2+} ions occurs to accommodate the creatinine molecule in the coordination sphere. Thus, the observed trend can be attributed to the kinetics of the convenient spatial rearrangement, which attains the most energetically favourable state at 5 minutes of reaction time. After this creatinine coordination process gets completed, the transformation of Co^{2+} to Co^{3+} gets either completed or attains certain equilibrium, and the oxidation current reverts to its original value.

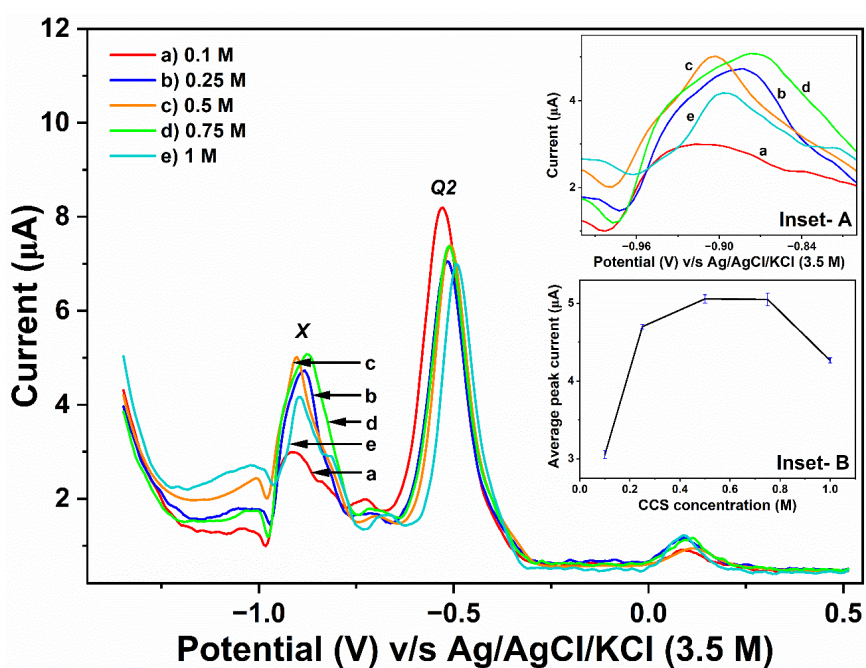


Figure 5.4: DPVs obtained for test solutions having different CCS concentrations. ('Inset- A' shows an enlarged view of peak X. 'Inset- B' represents the plot of peak X intensity v/s CCS concentration).

Figure 5.4 represents the DPVs of the test solutions having different concentrations of CCS while keeping the reaction time, CRS concentration and 2-NBA concentration fixed. From the calibration curve of the average oxidative peak current of X plotted against the concentrations of CCS, shown in Figure 5.4 (Inset- B), it was observed that the intensity of X initially increased as we increased the concentration of CCS from 0.1 M to 0.5 M, then remained stable up to 0.75 M, followed by a decrease. The initial increase can be attributed to the increase in the formation of Co^{2+} -2-NBA complex (and simultaneously, its electrochemical oxidation) with the increase in CCS concentration and the eventual decrease at higher concentrations of CCS can be attributed to the interruption caused by

the unreacted Co^{2+} ions on the electrochemical oxidation of Co^{2+} -2-NBA complex by hindering its movement towards the electrode surface.

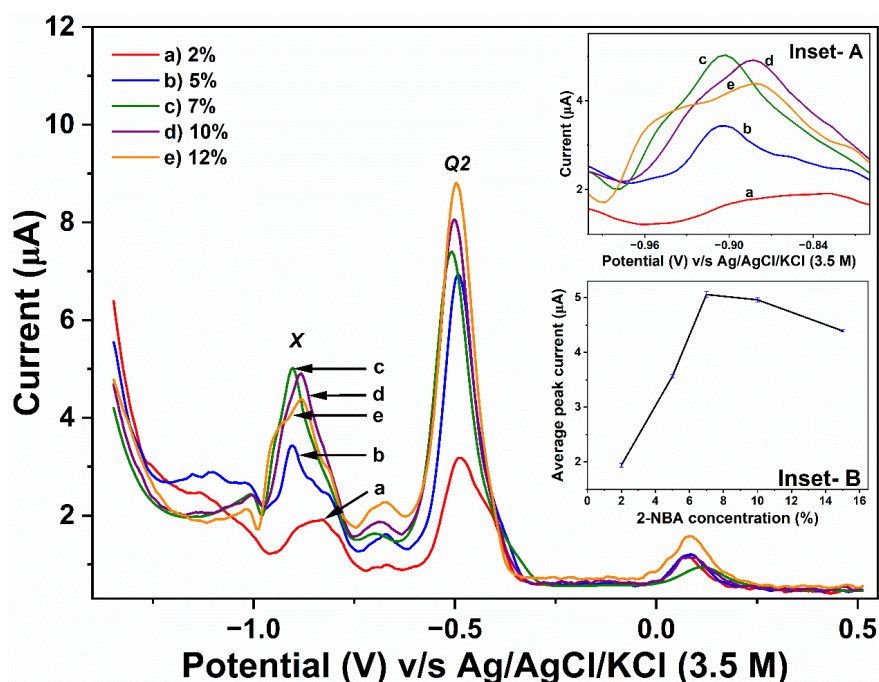


Figure 5.5: DPVs obtained for test solutions having different 2-NBA concentration. ('Inset- A' shows an enlarged view of peak X. 'Inset- B' represents the plot of peak X intensity v/s 2-NBA concentration).

Figure 5.5 represents the DPVs of test solutions having different concentrations of 2-NBA while keeping the reaction time, CRS concentration and CCS concentration fixed. From the calibration curve of the average oxidative peak current of X plotted against the concentrations of 2-NBA solution, shown in Figure 5.5 (Inset- B), it was observed that the intensity of X initially increased with the concentration of 2-NBA from 2 % to 7 % and thereafter, it showed a decreasing trend. This trend can also be explained by the initial increase in the formation of Co^{2+} -2-NBA complex (and simultaneously, its electrochemical oxidation) with the increase in NBS concentration until 7 %, and the gradual decrease thereafter can be attributed to the hindrance caused by unreacted 2-NBA molecule on the electrochemical oxidation of the complex, as discussed earlier.

The formation of the Co^{2+} -2-NBA and creatinine- Co^{3+} -2-NBA complexes have been explained in detail in section 5.3.6. However, from the optimization study, it can be concluded that 5 minutes of reaction time, 0.5 M concentration of CCS, and 7 % ethanolic

solution of 2-NBA were optimum conditions for the reaction between creatinine with 2-NBA and cobalt ions.

5.3.3 LOD determination

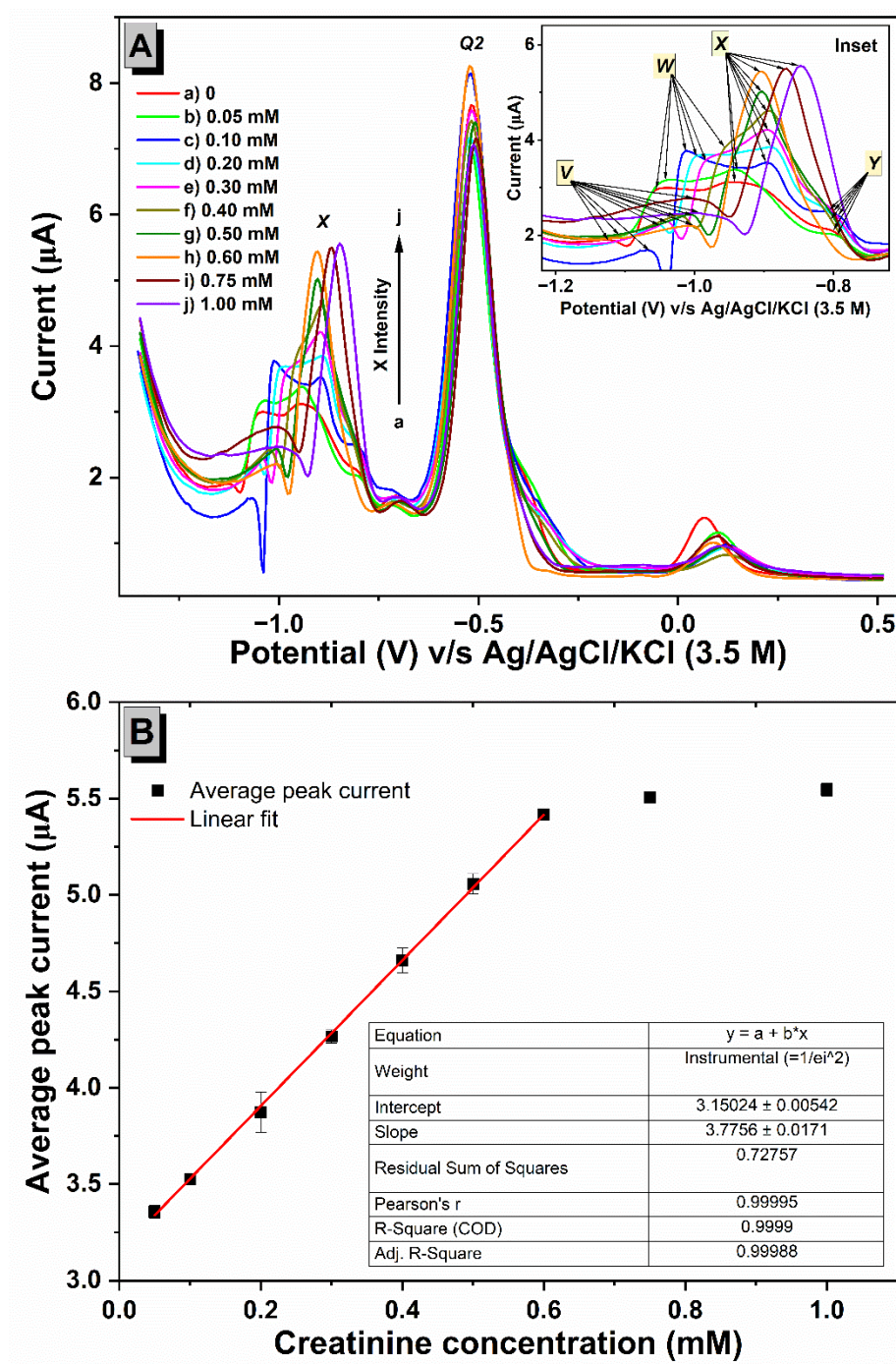


Figure 5.6: A) DPVs obtained for a) blank solution and (b-j) test solutions containing different CRS concentrations ('Inset' shows an enlarged view of the peaks V, W, X, and Y, for all the voltammograms). B) Calibration curve generated by plotting average peak currents of peak X against the different CRS concentrations.

Figure 5.6 (A) represents the DPVs of the blank and the test solutions. The test solutions were prepared with different CRS concentrations (0.05 mM to 100 mM). The correct designation of the peaks was important for the LOD determination and for deducing a plausible reaction mechanism (explained in Section 5.3.6). Hence, the shifting and/or masking of the peaks *V*, *W*, *X*, and *Y*, with the increasing creatinine concentration in the test solutions were noted, as shown in the 'Inset'. It was noticed that the peak *V* showed a gradual shift towards higher potential with an increasing creatinine concentration. In comparison with the blank solution, although the intensity of peak *V* is a little higher in the presence of creatinine, a quantitative increase in its intensity was not observed. Similarly, the peak *W* also exhibited a shift towards higher potential with increasing creatinine concentration. However, the intensity of *W* increased only until the CRS concentration in the test solution was increased to 0.10 mM. In the CRS concentration range between 0.10 mM to 0.40 mM, the intensity of *W* was found to be almost stable, and beyond 0.40 mM, the peak *W* couldn't be properly distinguished as it was masked due to the presence of a more intense peak (*X*) at the nearby potential. The low-intensity peak, *Y*, neither underwent any position shift nor exhibited any quantitative intensity variation with increasing creatinine concentration. Furthermore, beyond the CRS concentration of 0.50 mM, peak *Y* was also observed to get masked due to the presence of intense peak *X* at the nearby potential. Hence, peaks *V*, *W*, and *Y* were unsuitable for the quantitative determination of creatinine.

The peak *X* displayed a different trend. Initially, it exhibited a slight shift towards higher potential with increasing CRS concentration from 0 (in blank solution) to 0.20 mM. No change in its peak position was observed in the CRS concentration range of 0.20 to 0.60 mM. Beyond 0.60 mM, peak *X* showed a gradual shift towards the higher potential again. However, the intensity of peak *X* displayed a sensitive and quantitative increase for a large range with the increase in creatinine concentration, which was necessary for creatinine determination. Hence, the variation of peak *X* was chosen for LOD calculation.

In the plot of the average intensity of peak *X* against the concentrations of creatinine, as can be seen in Figure 5.6 (B), an excellent linearity with the R^2 value of 0.99 and slope of 3.78 was observed in the concentration range of 0.05 to 0.6 mM (50 μM to

600 μM). Beyond 0.6 mM, the graph indicated the attainment of saturation, as we further increased the concentration to 1 mM. The linear fit is represented by Equation 1.

$$y = 3.78x + 3.15 \quad (\text{Eq. 1})$$

The standard deviation (Sb) for the blank solution was obtained to be 0.012 and the system's LOD was determined to be 9.5 μM . Thus, this method can be well-utilised for serum creatinine determination.

5.3.4 Interference study

Some other blood components, such as uric acid, ascorbic acid, glucose, urea and albumin can act as interfering agents during creatinine detection. The variation in the intensity of peak X in the presence of different concentrations of these components mentioned above was checked. In serum, the normal concentration of uric acid varies in the range of 1.5–6.0 mg/dL for women and 2.5–7.0 mg/dL for men [5], the normal concentration of ascorbic acid varies in the range of 40–120 μM [6], the normal glucose level varies in the range of 80–120 mg/dL [7], the normal concentration of urea varies in the range of 3.3–6.7 mM [8] and normal albumin level varies from 3.5–5.0 g/dL [9]. The interference study was carried out by varying the concentration of these components, considering their respective normal pathological ranges.

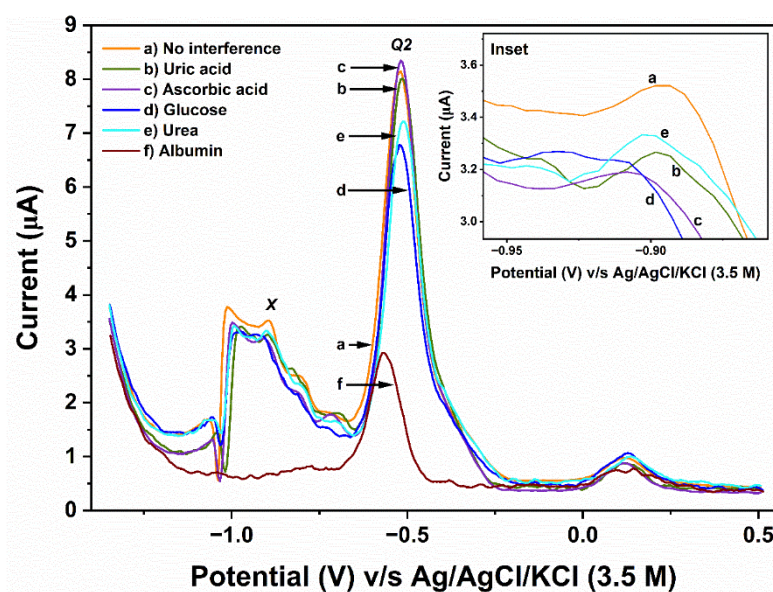


Figure 5.7: DPVs obtained for test solutions in the presence of a) no interference, b) 8 mg/dL uric acid, c) 150 μM ascorbic acid, d) 150 mg/dL glucose, e) 7 mM urea, and f) 5 g/dL albumin ('Inset' shows an enlarged view of the peak X in the voltammograms).

Figure 5.7 represents the DPVs obtained for the test solutions in the absence and presence of other blood components. In comparison with the interferent-free test solution, as can be seen in the figure, there was no change in the voltammogram pattern of the test solution spiked with uric acid, ascorbic acid, glucose or urea, although a slight reduction in the intensity of peak *X* was noticed. It is observed that in the selected potential window of this system, none of the added components underwent any electrochemical oxidation and no other electroactive species was generated by any chemical interaction of the added components with cobalt ions and/or 2-nitrobenzaldehyde, thus indicating high selectivity of the method. However, the voltammogram response differed in the presence of albumin and no peak of *X* was noticed, indicating a total interference by the protein molecule.

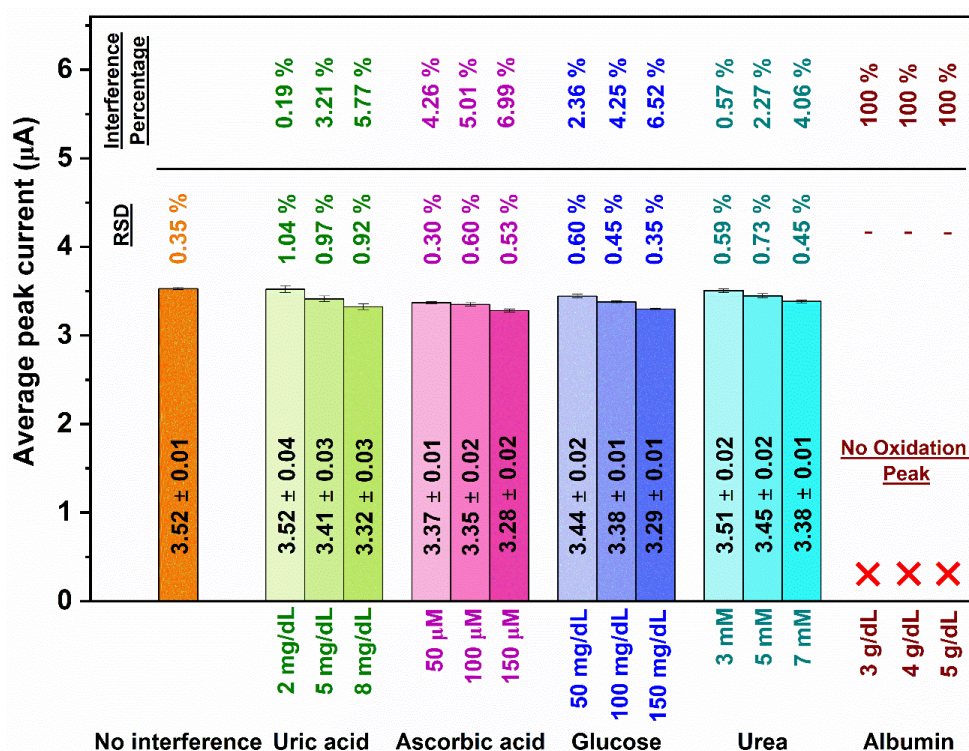


Figure 5.8: A bar diagram illustrating the average intensities of *X* with relative standard deviations, for test solutions in the absence and presence of varying concentrations of interfering components, and the interference percentage in each case.

The percentages of interference by different concentrations of uric acid, ascorbic acid, glucose, urea and albumin, have been highlighted in Figure 5.8. For the selected

concentrations of the interfering components, interference was in the range of 0.19–5.77 % in the presence of uric acid, 4.26–6.9 % in the presence of ascorbic acid, 2.36–6.52 % in the presence of glucose, 0.57–4.06 % in the presence of urea and 100 % in the presence of albumin. Thus, the system could be expected to be highly selective for determining creatinine in a protein-free serum sample.

5.3.5 Human blood serum (HBS) sample analysis and analytical performance of this method

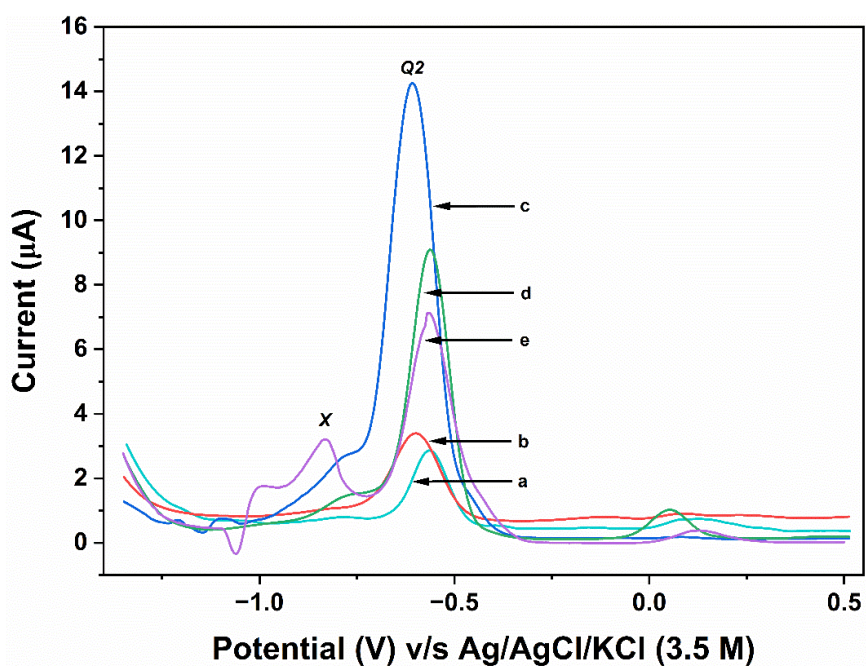


Figure 5.9: DPVs obtained for a) Albumin spiked 'CRS/2-NBA/CCS', b) Raw HBS + 2-NBA solution + CCS, c) ACN mixed 'CRS/2-NBA/CCS', d) 'ACN mixed deproteinized HBS' + 2-NBA solution + CCS, and e) 'ACN removed deproteinized HBS' + 2-NBA solution + CCS.

Some voltammograms were recorded to establish the interfering effect of albumin and ACN in HBS analysis, as shown in Figure 5.9. The voltammogram obtained for albumin spiked test solution (curve a) appeared similar to the voltammogram obtained for raw HBS after the addition of 2-NBA solution and CCS (curve b). While peak Q_2 appeared largely inhibited in the voltammograms, peak X wasn't observed. We believe that albumin caused the total interference of peak X in HBS, which was also proven in the interference study conducted in the buffer medium (Section 5.3.4). Therefore, deproteinization of the HBS was carried out via the ACN treatment described in Section 5.2.7.

It is also to be noted that the mixture of ACN and deproteinized HBS, obtained after removing the protein precipitate, cannot be considered for the analysis as ACN too inhibits the peak *X*. This can be comprehended from the voltammogram of ACN mixed test solution in 1:1 volume ratio, shown in Figure 5.9 (curve c) and the voltammogram of ‘ACN mixed deproteinized HBS’ after the addition of 2-NBA solution and CCS, shown in Figure 5.9 (curve d). While intense *Q2* peaks were observed in curves ‘c’ and ‘d’, peak *X* appeared masked. The *Q2* peak appeared more intense in the buffer medium (curve c) than in the deproteinized serum medium (curve d) in the presence of ACN. Interestingly, after ACN removal, peak *X* reappeared for the mixture of 6-fold diluted deproteinized HBS with 2-NBA solution and CCS (curve e). Hence, the ACN removal step from the mixture by incubating it at subzero temperature is a prime requisite.

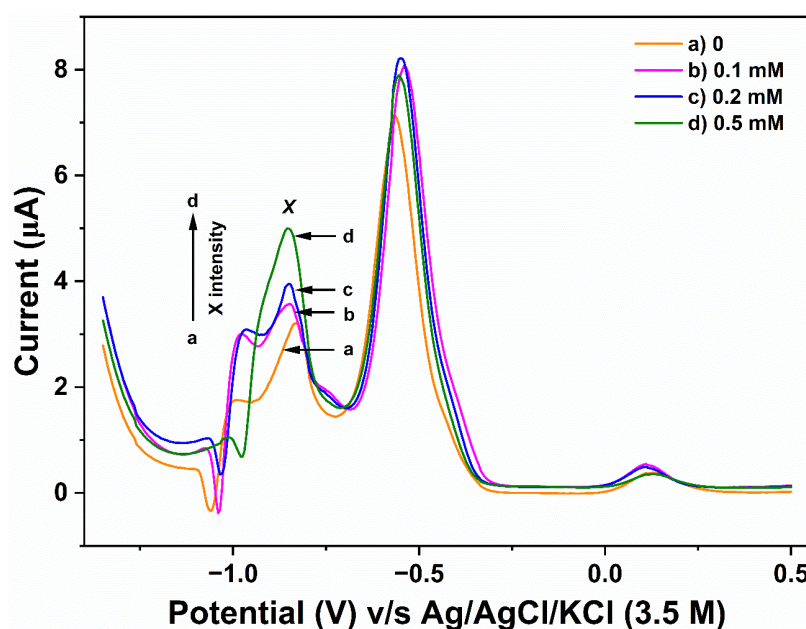


Figure 5.10: DPVs obtained for the deproteinized HBS spiked with a) 0, b) 0.1 mM, c) 0.2 mM and d) 0.5 mM creatinine, after adding CCS and 2-NBA solution.

Figure 5.10 shows the voltammograms obtained after the addition of 2-NBA solution and CCS to a 6-fold diluted deproteinized HBS sample, spiked with different creatinine concentrations. As can be seen in the figure, the intensity of peak *X* increased with the increasing concentration of spiked creatinine. The recovery percentage obtained in each case has been tabulated in Table 5.1.

Table 5.1: Recovery percentage of creatinine in spiked serum samples.

Spiked concentration (mM)	Obtained peak X current (10^{-2} μA)	Obtained concentration (10^{-3} mM)	A = Average obtained concentration (10^{-3} mM)	RSD (%)	E = Expected concentration (10^{-3} mM)	Average recovery percentage (%) = $(A/E)*100$ %
0	320.71	15.11	15.81	3.30	-	-
	321.18	16.35				
	321.04	15.98				
0.1	357.09	111.35	111.55	1.80	115.81	96.32
	358.13	114.10				
	356.28	109.21				
0.2	393.83	208.54	214.12	2.04	215.81	99.22
	397.87	219.23				
	396.12	214.60				
0.5	497.51	482.83	488.19	1.81	515.81	94.65
	496.86	481.11				
	504.24	500.63				

From Table 5.1, it can be known that the recovery percentage of creatinine was found to be in the range of 94.65 % to 99.22 % for the spiked serum samples studied. Hence, it can be stated that the system exhibits a very good sensitivity. The average oxidative peak current of X for the non-spiked serum sample was found to be 3.21 ± 0.002 μA . Considering the dilution factor, the creatinine concentration in the serum sample was calculated to be 94.87 μM (1.07 mg/dL), which is within the normal range.

A comparison of the analytical performance of this method with the contemporary electrochemical methods is shown in Table 5.2.

Table 5.2: Comparison of some electrochemical creatinine detection methods.

Sl. No.	Detection Technique	Electrode	Linear detection range	R^2 value	LOD (μM)	Demonstrated in-	Reference
---------	---------------------	-----------	------------------------	-------------	-----------------------	------------------	-----------

1.	CV	Glassy carbon macrodisk	0-10	> 0.99	35	-	[10]
2.	CV	SB3C16@ Cu_2O modified screen printed carbon electrode	0.01-0.2	0.9876	5	Serum	[11]
3.	DPV	Carbon black- Fe^{3+} solution doped carbon paper disk	0.10-6.50	0.993	43	Urine	[12]
4.	LSV	Pt microelectrode arrays	0-5	-	59	Synthetic urine	[13]
5.	CV	Au-Ag modified glassy carbon electrode	-	0.998	800	Artificial urine	[14]
6.	CV	CuO-IL/rGO modified 3D printed electrode	500-35000	0.999	37.2	Urine	[15]
7.	DPV	Enzymes immobilised $\text{Re}_x\text{Bi}_{1-x}\text{-O}$ coated ITO	0.05-2	0.99	28	Serum	[16]
8.	DPV	Bare glassy carbon electrode	1-25	0.994	500	Urine	[17]
9.	DPV	Bare glassy carbon electrode	0.05-0.6	0.999	9.5	Deproteinized Serum	This work

From Table 5.2, it can be seen that the LOD of our method is lower than most of the recently reported detection methods.

5.3.6 Plausible mechanistic pathway: a discussion

5.3.6.1 From the electrochemical perspective

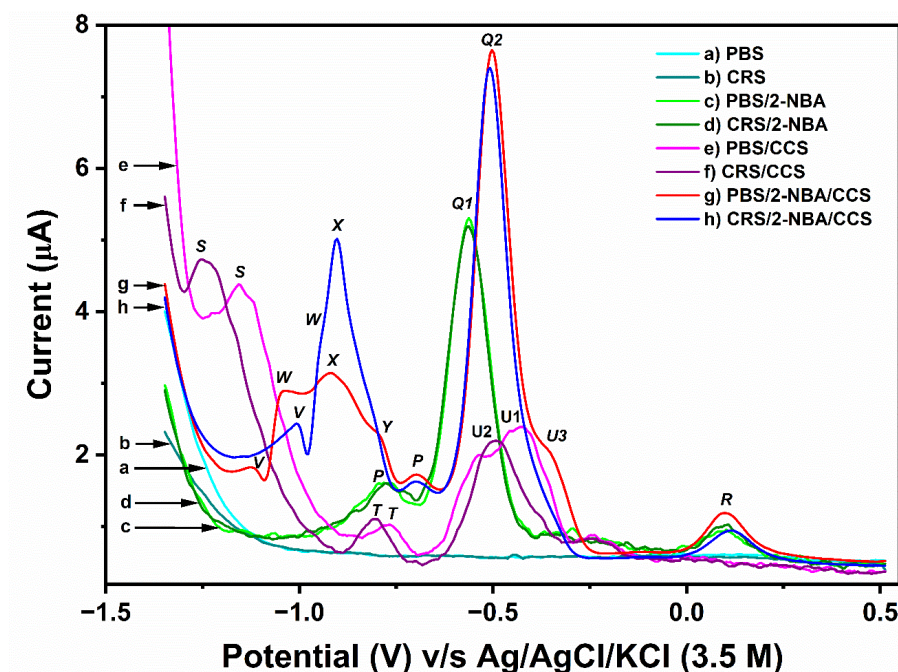


Figure 5.11: DPVs obtained for a) PBS, b) CRS, c) PBS/2-NBA, d) CRS/2-NBA, e) PBS/CCS, f) CRS/CCS, g) blank solution (PBS/2-NBA/CCS), and h) test solution (CRS/2-NBA/CCS).

Figure 5.11 represents the DPVs of different solutions and solution mixtures involved in the analysis procedure. It is seen that no redox peak is obtained for PBS (curve a) and CRS (curve b). However, three oxidation peaks, *P* (-0.77 ± 0.002 V), *Q1* (-0.56 ± 0.002 V), and *R* (0.9 ± 0.001 V), were obtained for the PBS/2-NBA (mixture of PBS and 2-NBA solution), and CRS/2-NBA (mixture of 0.5 mM CRS and 2-NBA solution), as can be seen in curve 'c' and 'd', respectively. These are the native peaks of 2-NBA. While peak *Q1* is a prominent peak observed due to $1e^- - 1H^+$ transfer from the nitro group of the protonated 2-NBA (Path- A, Scheme 5.1), the other two low-intensity peaks (*P* and *R*) are due to electron transfer from the carbonyl group of 2-NBA [17]. These two DPV curves infer that there is no chemical reaction between creatinine and 2-NBA in the PBS medium.

The low-intensity peaks (*P* and *R*) do not have any quantitative correlation with the analyte (creatinine) and are discarded in the subsequent discussion.

In the DPV of PBS/CCS (mixture of PBS and CCS), two prominent oxidation peaks, *S* (-1.15 ± 0.003 V) and *UI* (-0.41 ± 0.002 V), along with a low-intensity peak, *T* (-0.76 ± 0.003 V), were seen (curve e). Following the results of our previous work [49], it can be inferred that these are the native peaks of cobalt ions. While the first prominent peak, *S*, can be assigned for the dissolution of Co^0 from the electrode surface to produce Co^{2+} , the second prominent peak, *UI*, can be assigned for the $\text{Co}^{2+}/\text{Co}^{3+}$ redox process involving free cobalt ions in the PBS medium (Path- B, Scheme 5.1). The low-intensity peak, *T*, can be assigned for the oxidation of cobalt-oxide formed in the solution.

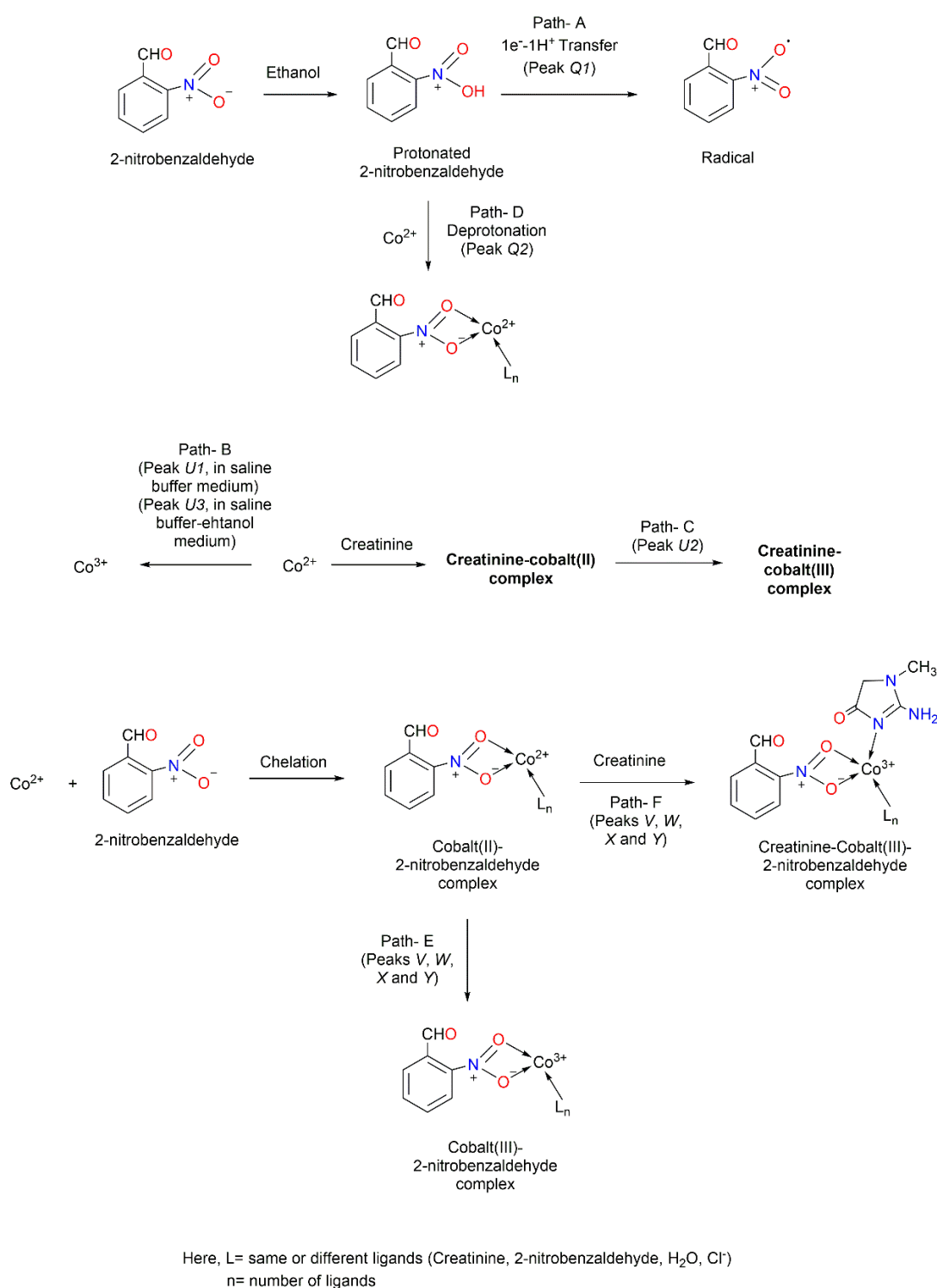
Although the peaks *S* and *UI* were prominently observed, peak *S* appeared a little distorted while peak *UI* appeared distorted and broad. *S* and *UI* also appeared at lower potentials, compared to their corresponding peaks obtained in the aqueous medium [18] which can be attributed to the solvent effect.

DPV behaviour of CRS/CCS (mixture of 0.5 mM CRS and CCS), as shown in curve 'f', is almost the same as CCS/PBS, except for slight peak shifts towards lower potentials. These shifts can be attributed to the complex formation between creatinine and Co^{2+} (creatinine- Co^{2+}). Hence, the peak, *U2* (-0.49 ± 0.002 V), in CRS/CCS can be assigned for the $\text{Co}^{2+}/\text{Co}^{3+}$ redox process (Path- C, Scheme 5.1) involving the creatinine-coordinated cobalt ions. A little increase in the intensity of peak *S* (-1.25 ± 0.003 V) was also observed which can be attributed to a higher degree of Co^0 dissolution to form Co^{2+} , owing to the coordination affinity of creatinine with Co^{2+} ions. This observation also infers that although the creatinine- Co^{2+} complexation is possible in CRS/CCS, this reaction is of no new redox significance as compared to PBS/CCS.

In the blank solution (mixture of PBS, 2-NBA solution, and CCS), the prominent native peaks of protonated 2-NBA (*Q1*) and cobalt ions (*S* and *UI*) would have appeared, had there been no interaction between cobalt ion and 2-NBA. However, while *S* and *Q1* did not show up, *UI* appeared at a shifted position as *U3* (-0.35 ± 0.002 V). Additionally, some new peaks, *V* (-1.12 ± 0.003 V), *W* (-1.04 ± 0.003 V), *X* (-0.91 ± 0.001 V), *Y* (-0.79 ± 0.002 V) and *Q2* (-0.50 ± 0.002 V) appeared as can be seen in curve 'g'. It is to be noted that peak *Q2* appeared as the most intense peak, while peak *U3* appeared as a shoulder

peak. All these observations can be explained by the chelation property of the cobalt ion with the nitro group of 2-NBA, as reported earlier [18]. In the water-ethanol medium, the formation of a water-soluble 7-coordinated $[\text{Co}(\text{creatinine})_3(\text{H}_2\text{O})_2(2\text{-NBA})]\text{Cl}_3$ complex having Co^{3+} was reported [18]. However, in the saline buffer-ethanol medium, the number of secondary ligands and the possibility of involvement of other ligands like Cl^- in the coordinating sphere cannot be ruled out. Hence, peaks *V*, *W*, *X*, and *Y* can be assigned to the oxidation peaks corresponding to the $\text{Co}^{2+}/\text{Co}^{3+}$ redox couple (Path E, Scheme 5.1), where cobalt ions are coordinated with 2-NBA and diverse secondary ligands, giving rise to distinct species with varying secondary ligand arrangements and numbers. On the other hand, peak *Q2* can be assigned to the deprotonation from the protonated nitro-group of the unreacted 2-NBA (Path- D, Scheme 5.1) to chelate with the Co^{2+} ions. The generation of the more intense *Q2* instead of *Q1* in the presence of cobalt ions indicates the preferential deprotonation of protonated 2-NBA molecules facilitated by Co^{2+} ions over the $1\text{e}^- - 1\text{H}^+$ transfer. The shoulder peak *U3* in the blank solution can be attributed to the $\text{Co}^{2+}/\text{Co}^{3+}$ redox process (Path B, Scheme 5.1) involving unreacted free Co^{2+} ions in the saline buffer-ethanol medium.

In the test solution (mixture of 0.5 mM CRS, 2-NBA solution, and CCS), as can be seen in curve 'h', while the peaks *V* (-1.00 ± 0.003 V), *X* (-0.90 ± 0.001 V) and *Q2* (-0.50 ± 0.02 V) appeared well-resolved, the peaks *W* and *Y* appeared masked (explained in Section 5.3.3). In comparison with the blank solution (curve 'g'), no change in the intensity of peak *Q2* was observed in the voltammogram of the test solution, inferring that the deprotonation step was not affected by the presence of creatinine. The peak *U3* was also not observed for the test solution, indicating that there was no free Co^{2+} ion in the presence of creatinine due to complexation. However, apart from the shifting in peak potentials, the intensity of peaks *V* and *X* showed an increase in their respective intensities. Thus, it can be inferred that in the presence of creatinine, electrooxidation of Co^{2+} to Co^{3+} in the cobalt-2-NBA complex (Path F, Scheme 5.1) gets enhanced, due to better stabilization of Co^{3+} through the formation of some complexes like $[\text{Co}(\text{creatinine})_3(\text{H}_2\text{O})_2(2\text{-NBA})]\text{Cl}_3$ obtained in aqueous medium [18]. It was reported that the oxidation state of cobalt ion in $[\text{Co}(\text{creatinine})_3(\text{H}_2\text{O})_2(2\text{-NBA})]\text{Cl}_3$ obtained in aqueous medium is +3 [18]. The detailed electrochemical reaction pathways are shown in Scheme 5.1.



Scheme 5.1: Electrochemical redox processes occurring in the reaction between cobalt ions, creatinine, and 2-nitrobenzaldehyde.

5.3.6.2 From the spectroscopic perspective

UV-visible spectroscopy of some solutions and solution mixtures with appropriate baseline correction, as represented by Figure 5.12, was also recorded to gather some more supportive evidence for the proposed mechanistic route. While the UV-visible spectra of CRS, PBS/CCS, and CRS/CCS were carried out with PBS as the baseline, the same of PBS/2-NBA, CRS/2-NBA, blank solution, and test solution were recorded with the mixture of PBS and ethanol as the baseline.

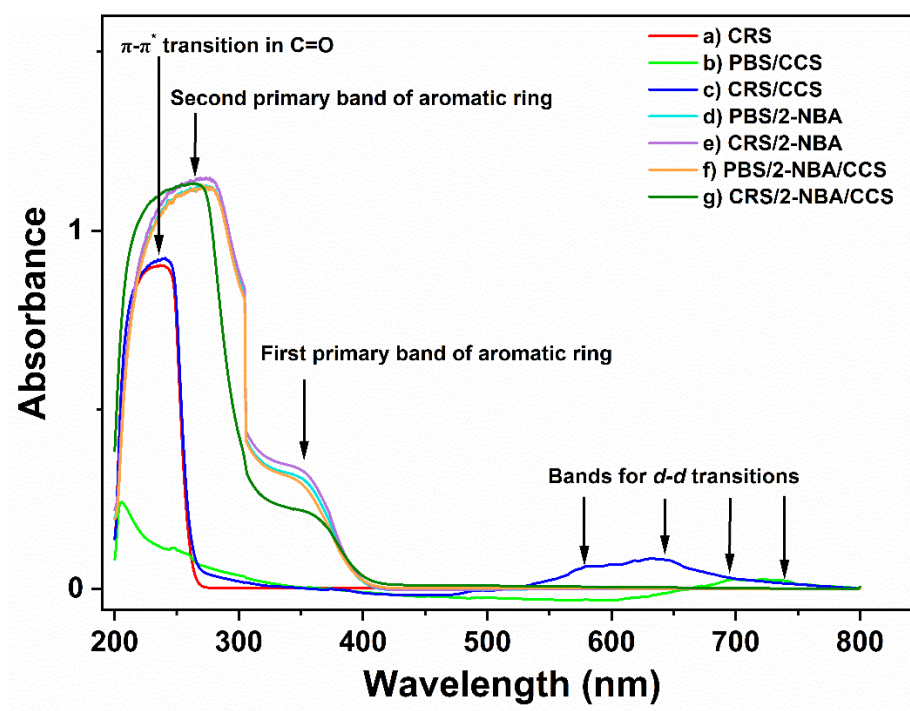


Figure 5.12: UV-visible spectra obtained for a) CRS, b) PBS/CCS, c) CRS/CCS, d) PBS/2-NBA, e) CRS/2-NBA, f) blank solution (PBS/2-NBA/CCS), and g) test solution (CRS/2-NBA/CCS).

As can be seen in the UV-visible spectrum of CRS (curve a), a broad band at 235 nm was observed for $\pi-\pi^*$ transition in the carbonyl group of creatinine [19]. In the spectra of PBS/CCS, broad low-intensity bands for spin-forbidden $d-d$ transitions in the free Co^{2+} ions at 698 nm and 738 nm were observed [20]. However, in the spectrum of CRS/CCS (curve 'c'), absorption bands due to both $\pi-\pi^*$ transition (at 235 nm) and $d-d$ transitions (at 582 nm and 639 nm) were observed. The $\pi-\pi^*$ transition in CRS/CCS was found to occur at the same λ_{max} as in CRS, suggesting that this is due to the presence of unreacted creatinine. However, compared to PBS/CCS, the $d-d$ transitions in CRS/CCS exhibited

wavelength shifts, likely resulting from alterations in the ligand field environment caused by the formation of a creatinine- Co^{2+} complex.

In the spectrum of PBS/2-NBA (curve 'd'), primary bands due to $\pi\text{-}\pi^*$ transition in the aromatic ring of 2-NBA were observed. A similar spectrum was also observed for CRS/2-NBA (curve 'e') as the broader primary bands of 2-NBA masked the band due to $\pi\text{-}\pi^*$ transition in the C=O group of creatinine.

The primary bands further persisted in the spectrum of the blank solution (curve 'f'), which hinted at the non-involvement of the aromatic ring of 2-NBA in any chemical interaction with Co^{2+} ions. However, no bands due to $d\text{-}d$ transitions were observed in the blank solution, which can be attributed to either the solvent (PBS + ethanol) effect or the chelation of Co^{2+} ions with the nitro group of 2-NBA.

In the test solution (curve g), the presence of both the Co^{2+} -2-NBA (unreacted) complex and creatinine- Co^{3+} -2-NBA (after reaction) complex was expected. No occurrence of any band due to $d\text{-}d$ transitions for either of the cobalt ions and the masking of the $\pi\text{-}\pi^*$ transition band of the C=O group of creatinine, as observed in the spectrum of test solution, can be attributed to the same chelation or solvent effect as mentioned above. It was earlier reported that the creatinine- Co^{3+} -2-NBA complex has a graphitic structure due to the stacking of their aromatic rings with $\pi\text{-}\pi$ interaction [18], which explained the lowering of the intensity of the first primary band and narrowing of the second primary band in the test solution, as compared to its corresponding intensities in PBS/2-NBA, CRS/2-NBA and the blank solution.

5.4 Conclusion

In this study, we have developed an electrochemical determination method of creatinine in human blood serum across its entire pathological range, using cobalt ions and 2-nitrobenzaldehyde. The differential pulse voltammetry technique was enabled as the transduction system and the mechanism of the method is based on the preferential conversion of the Co^{2+} -2-nitrobenzaldehyde complex to creatinine- Co^{3+} -2-nitrobenzaldehyde complex in the presence of creatinine. Comparing the voltammogram responses by varying the reaction time and reagent compositions, the reaction time of 5 minutes, cobalt concentration of 0.5 M and 2-nitrobenzaldehyde concentration of 7 % (weight/volume in ethanol) were determined as the optimum parameters for the method.

At the optimum conditions, the LOD of the system was determined to be $9.5 \mu\text{M}$ and the system exhibited excellent linearity in the concentration range of $50 \mu\text{M}$ to $600 \mu\text{M}$, with an R^2 value of 0.99. The interference study revealed that most of the common serum components (uric acid, glucose, urea and ascorbic acid) exhibited no significant interference in the method. However, interference in the result was caused by albumin. Remarkable selectivity of this method can be achieved in serum by deproteinizing the serum via centrifugating it with acetonitrile, followed by its incubation at subzero temperature to separate acetonitrile. Thus, the method was successfully demonstrated in deproteinized human serum and the experimentally determined creatinine recovery percentages between 94.65–99.22 % indicated its high sensitivity. Corroborated with electrochemical DPV and UV-vis analysis, a plausible mechanism of the reaction between creatinine, cobalt ion and 2-nitrobenzaldehyde has also been proposed, designating all the electrochemical oxidation peaks. This proposed method demonstrated better analytical performance than many contemporary methods, showcasing its potential as a promising new tool for creatinine determination in human blood serum.

References

- [1] Muralidharan, S., Nagaraja, K. S. and Udupa, M. R. Cobalt (II) complexes of creatinine. *Transition Metal Chemistry*, 9:218–220, 1984.
- [2] El-Sayed, M. Y., Refat, M. S., Altalhi, T., Eldaroti, H. H. and Alam, K. Preparation, spectroscopic, thermal and molecular docking studies of covid-19 protease on the manganese (II), iron (III), chromium (III) and cobalt (II) creatinine complexes. *Bulletin of the Chemical Society of Ethiopia*, 35(2):399–412, 2021.
- [3] Dasgupta, P., Kumar, V., Krishnaswamy, P. R. and Bhat, N. Biochemical assay for serum creatinine detection through a 1-methylhydantoin and cobalt complex. *RSC Advances*, 10(64):39092–39101, 2020.
- [4] Yoshida, M., Akane, A., Nishikawa, M., Watabiki, T. and Tsuchihashi, H. Extraction of thiamylal in serum using hydrophilic acetonitrile with subzero-temperature and salting-out methods. *Analytical Chemistry*, 76(16):4672–4675, 2004.
- [5] Wang, Q., Wen, X. and Kong, J. Recent progress on uric acid detection: a review. *Critical Reviews In Analytical Chemistry*, 50(4):359–375, 2020.

- [6] Kumar, S., Singh, R., Yang, Q., Cheng, S., Zhang, B. and Kaushik, B. K. Highly sensitive, selective and portable sensor probe using germanium-doped photosensitive optical fiber for ascorbic acid detection. *IEEE Sensors Journal*, 21(1):62–70, 2020.
- [7] Yu, Q., Jiang, J., Chen, Z., Han, C., Zhang, X., Yang, S., Zhou, P., Deng, T. and Yu, C. A multilevel fluorometric biosensor based on boric acid embedded in carbon dots to detect intracellular and serum glucose. *Sensors and Actuators B: Chemical*, 350:130898, 2022.
- [8] Pundir, C. S., Jakhar, S. and Narwal, V. Determination of urea with special emphasis on biosensors: A review. *Biosensors and Bioelectronics*, 123:36–50, 2019.
- [9] Zhu, L., Chen, M. and Lin, X. Serum albumin level for prediction of all-cause mortality in acute coronary syndrome patients: a meta-analysis. *Bioscience reports*, 40(1):BSR20190881, 2020.
- [10] Ngamchuea, K., Wannapaiboon, S., Nongkhunsan, P., Hirunsit, P. and Fongkaew, I. Structural and electrochemical analysis of copper-creatinine complexes: application in creatinine detection. *Journal of The Electrochemical Society*, 169(2):020567, 2022.
- [11] Rakesh Kumar, R. K., Shaikh, M. O., Kumar, A., Liu, C. H. and Chuang, C. H. Zwitterion-functionalized cuprous oxide nanoparticles for highly specific and enzymeless electrochemical creatinine biosensing in human serum. *ACS Applied Nano Materials*, 6(3):2083–2094, 2023.
- [12] Fava, E. L., do Prado, T. M., Garcia-Filho, A., Silva, T. A., Cincotto, F. H., de Moraes, F. C., Faria, R. C. and Fatibello-Filho, O. Non-enzymatic electrochemical determination of creatinine using a novel screen-printed microcell. *Talanta*, 207:120277, 2020.
- [13] Kaewket, K. and Ngamchuea, K. Electrochemical detection of creatinine: exploiting copper (ii) complexes at Pt microelectrode arrays. *RSC Advances*, 13(47):33210–33220, 2023.
- [14] Nene, A., Phanthong, C., Surareungchai, W. and Somasundrum, M. Electrochemical detection of creatinine using Au–Ag bimetallic nanoparticles. *Journal of Solid State Electrochemistry*, 27(10):2869–2875, 2023.

- [15] Teekayupak, K., Aumnate, C., Lomae, A., Preechakasedkit, P., Henry, C. S., Chailapakul, O. and Ruecha, N. Portable smartphone integrated 3D-Printed electrochemical sensor for nonenzymatic determination of creatinine in human urine. *Talanta*, 254:124131, 2023.
- [16] Das, M., Chakraborty, T. and Kao, C. H. Sol-gel synthesized $\text{Re}_x\text{Bi}_{1-x}\text{O}$ thin films for electrochemical creatinine sensing: A facile fabrication approach. *Materials Chemistry and Physics*, 315:128889, 2024.
- [17] Hussain, N. and Puzari, P. A novel method for electrochemical determination of creatinine in human urine based on its reaction with 2-nitrobenzaldehyde using a glassy carbon electrode. *Journal of Applied Electrochemistry*, 54(1):175–187, 2024.
- [18] Hussain, N. and Puzari, P. Deciphering the complexation processes of creatinine-cobalt and creatinine-cobalt-2-nitrobenzaldehyde: Morphological, spectroscopic and electrochemical analysis. *Journal of Molecular Structure*, 1316:139042, 2024.
- [19] Pavia, D. L., Lampman, G. M., Kriz, G. S., and Vyvyan, J. R. *Introduction to spectroscopy*. Cengage Learning, Boston, MA, 2008.
- [20] Vraneš, M., Gadžurić, S. B., Zsigrai, I. J. and Dožić, S. Absorption spectra of cobalt (II) chloride and nitrate complexes in aqueous calcium nitrate–ammonium nitrate melts: The influence of solvent composition. *Journal of Molecular Liquids*, 152(1-3):3438, 2010.